Available online at www.elixirpublishers.com (Elixir International Journal)

Vibrational Spectroscopy

Elixir Vib. Spec. 95 (2016) 40870-40880

ISSN: 2229-712X

Vibrational Spectral Studies, HOMO−LUMO, Thermodynamic Properties and Electrostatic Potential Surface Analysis of 3-Amino-4-Methyl Benzoic Acid Based on Density Functional Theory

M. Murugan[1], V. Balachandran[2], M.Karnan[3], MK.Murali[4] and A.Lakshmi[1]

[1]Department of Physics, Government Arts College, Tiruchirappalli 620 022, India.
[2]Department of Physics, A A Government Arts College, Musiri 621 211, India.
[3]Department of Physics, Srimad andavan Arts & Science College, Tiruchirappalli 620 005, India.
[4]Department of Physics, JJ College of Arts & Science , Pudukkottai 622 422, India.

ARTICLE INFO

Article history:
Received: 23 April 2016;
Received in revised form:
3 June 2016;
Accepted: 8 June 2016;

Keywords
FTIR spectra,
FT-Raman spectra,
3-amino-4-methyl benzoic acid,
Natural Bond Orbitals (NBO),
HOMO-LUMO.

ABSTRACT

The FT-Raman and FTIR spectra for 3-amino-4-methyl benzoic acid (AMBA) have been recorded in the region 4000–100 cm^{-1} and compared with the harmonic vibrational frequencies calculated by DFT method using B3PW91/6-31+G(d,p) and B3PW91/6-311++G(2d,2p) basis set with appropriate scale factors. IR intensities and Raman activities are also calculated by DFT methods. Optimized geometries of the molecule have been interpreted and compared with the reported experimental values for benzoic acid and some substituted benzoic acids. Furthermore, the molecular orbital calculations such as natural bond orbitals (NBO), HOMO-LUMO energy gap and Mapped molecular electrostatic potential (MEP) surfaces were also performed with the same level of DFT. The detailed interpretation of the vibrational spectra has been carried out with the aid of potential energy distribution (PED) results obtained from MOLVIB program.

1.Introduction

Derivatives of benzoic acid have been the subject of investigation for many reasons. A derivative of benzoic acid is an essential component of the Vitamin B complex. Benzoic acid occurs widely in plants and animals tissues along with Vitamin B complex and is used in miticides, contrast media in urology, cholocystrographic examinations and in the manufacture of pharmaceuticals.

As a result, there are many heterocyclic compounds have been investigated for anti inflammatory activity and suppressing side effects by these drugs is a challenge for many years [1,2]. A recent patent reported that benzoic acid derivatives have good anti-tumor properties and their activity being related to novel synergistic compositions that selectively control tumor tissue [3].

Benzoic acid, the simplest aromatic carboxylic acid containing carboxyl group bonded directly to benzene ring, is a white, crystalline organic compound; slightly soluble in water, soluble in ethanol, very slightly soluble in benzene and acetone. Its aqua solution is weakly acidic. It occurs naturally in many plants and resins. Benzoic acid is also detected in animals. The most of commercial benzoic acid is produced by the reaction of toluene with oxygen at temperatures around 200 C in the liquid phase and in the presence of cobalt and manganese salts as catalysts. It can be prepared also by the oxidation of benzene with concentrated sulphuric acid or carbon dioxide in the presence of catalysts. It is used as a rubber polymerization activators and retardants. Benzoic acid is converted to its salts and esters for the use of preservative application in foods, drugs and personal products. Amino group substituted benzoic acid at ortho position, is used as an intermediate for production of dyes, pigments and saccharin. It has amino and carboxylic group attached in ring structure. It and its esters are used in preparing perfumes, pharmaceuticals.

Benzoic acid is used as an intermediate for polymer stabilizers, pesticides, light sensitive compounds, animal feed supplements and other pharmaceuticals, pigments and dyestuff. There are almost infinite esters obtained from thousands of potential starting materials. Esters are formed by removal of water from an acid and an alcohol, e.g., carboxylic acid esters, phosphoric acid esters, and sulfonic acid esters. Carboxylic acid esters are used as in a variety of direct and indirect applications.

They are also used as intermediates for the manufacture of a variety of target com pounds. Because of its wide applications, the surface enhanced Raman scattering studies [4], vibrational spectra of benzoic acid [5] and methyl derivatives have been extensively investi gated.

To the best of our knowledge, neither quantum chemical calculations, nor the vibrational spectra have been reported, as yet. This inadequacy observed in the literature encouraged us to make this theoretical and experimental vibrational spectroscopic research based on the structure of molecules to give a correct assignment of the fundamental bands in experimental FT-IR and FT-Raman spectra. The entire scaled quantum mechanical method and density force fields calculations are performed by combining the experimental and theoretical aspects of Pulay and Rauhut [6]. Their training set and test set have been used to check the reliability of fitting. The overall scaling factors for theoretical harmonic frequencies have been verified with least-square fits [7]. The assignments have also been supported by the potential energy

Tele:
E-mail address: phymurugan@gmail.com

distribution, which is part of the outcomes of the normal coordinate analyses.

2. Experimental details

The sample 3-amino-4-methyl benzoic acid in the liquid form was provided by the Lancaster Chemical Company, (UK) with a purity of greater than 98% and it was used as such without further purification. The FTIR spectrum of 3-amino-4-methyl benzoic acid was recorded in the frequency region 4000–400 cm^{-1} on a NEXUS 670 spectrophotometer equipped with an MCT detector, a KBr pellet technique. The FT Raman spectrum of 3-amino-4-methyl benzoic acid was also recorded in the frequency region 3500–100 cm^{-1} on a NEXUS 670 spectrophotometer equipped with Raman module accessory with Nd:YAG laser operating at 1.5W power continuously with 1064 nm excitation.

3. Computational methods

For a supportive evidence to the experimental observations, the density functional theory (DFT) computations were performed with the aid of GAUSSIAN 09W software package [8] with internally stored B3PW91/6-31+G(d,p) and B3PW91/6-311++G(2d,2p) basis set methods. At first, the global minimum energy structure of the title molecule was optimized by both the aforesaid basis set. Subsequently the vibrational normal mode wavenumbers in association with the molecule were derived along with their IR intensity and Raman activity.

In our calculations, there were some deviations persist between the observed and calculated wavenumbers due to the neglect of anharmonic effect at the beginning of frequency calculation and basis set deficiencies. In the present study, these deviations were overcome by a selective scaling procedure in the natural internal coordinate representation followed by the reference [6,9]. Transformations of the force field and the subsequent normal coordinate analysis including the least squares refinement of the scaling factors, calculation of PED, IR and Raman intensities were done on a PC with the MOLVIB program (Version V7.0-G77) written by Sundius [10–11]. The PED elements provide a measure of each internal coordinate's contribution to the normal coordinate. For the plots of simulated IR and Raman spectra, pure Lorentzian band shapes were used with a bandwidth of 10 cm^{-1} and the modified Raman activities during scaling procedure with MOLVIB were converted to relative Raman intensities using the following relationship derived from the basic theory of Raman scattering [13–15].

$$I_i = \frac{f\left(\upsilon_0 - \upsilon_i\right)^4 S_i}{\upsilon_i\left[1 - \exp\left(\frac{-hc\upsilon_i}{kT}\right)\right]}$$

where υ_0 is the exciting wavenumber (1064 nm = 9398 cm^{-1}) of laser light source used while recording Raman Spectra, υ_i the vibrational wavenumber of the i^{th} normal mode. h, c and k_b fundamental constants, and f is a suitably chosen common normalization factor for all peak intensities of the Raman spectrum of the title molecule. Finally, the converted Raman intensities and the calculated infrared intensities were modified by assigning the highest intensity peak to 100%.

In order to predict the reactive behavior of a molecule, we have plotted MEP surface and derived electrostatic potential values and point charges at B3PW91/6-311++G(2d,2p) basis set. The population of atomic charges on the individual atoms and the distribution of atomic charges in core and valance were also derived using NBO calculations in GAUSSIAN 09W. From the computed NBO results, the stabilization energies of molecular species which are most responsible for the stability of molecule were identified. Furthermore, the highest occupied molecular orbital (HOMO) and the lowest unoccupied molecular orbital (LUMO) energies were predicted to interpret the orbital overlapping and the possibility of charge transfer within the molecule using B3PW91/6-311++G(2d,2p)) method and basis set combination. Apart from the aforesaid calculations, certain thermodynamic properties were computed at B3PW91/6-311++G(2d,2p) method to examine the intensity of molecular vibrations at different temperatures.

4. Results and discussion

4.1. Molecular geometry

The molecular structure of the AMBA belongs to CS point group symmetry. The optimized molecular structure of title molecule is obtained from GAUSSAN 09W and GAUSSVIEW programs are shown in Fig. 1. The molecule contains C=O, C-OH, NH_2 and CH3 connected with benzene ring. The experimental and calculated FTIR spectra of AMBA are given in Fig. 2. Fig. 3 represents the observed and calculated FTIR spectra of AMBA. The comparative optimized structural parameters such as bond lengths, bond angles and dihedral angles are presented in Table 1. From the theoretical values, it is found that most of the optimized bond lengths are slightly larger than the experimental values, due to that the theoretical calculations belonging to isolated molecules in gaseous phase while the experimental results belong to molecules in solid state [16]. Comparing bond angles and lengths of B3BY91with those of 6-31+G (d, p) and 6-311++G (2d, 2p)basis sets.

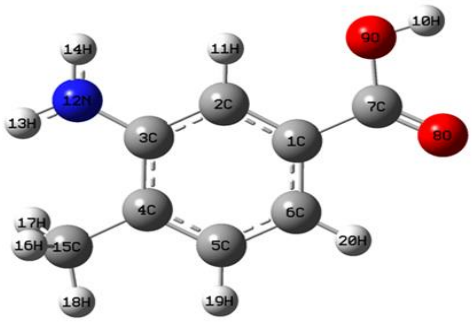

Fig 1. Optimized molecular structure of 3-amino-4-methyl benzoic acid.

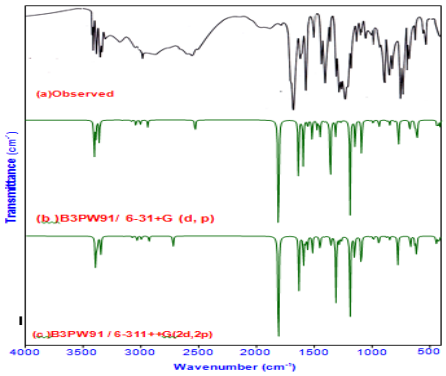

Fig2. FT IR spectrum of 3-amino-4-methyl benzoic acid (a) Observed (b) B3PW91/ 6-31+G (d, p) and (c) B3PW91 / 6-311++G(2d,2p).

Table 1.Optimized geometrical parameters of 3-amino-4-methyl benzoic acid based on B3PW91 / 6-31+G (d, p) and B3PW91 / 6-311++G(2d,2p).

Parameters	B3PW91 / 6-31+G (d,	B3PW91 / 6-311++G(2d,2p)	Exp[a]	Parameters	B3PW91 / 6-31+G (d,	B3PW91 / 6-311++G(2d,2p)	Exp[a]
C1-C2	1.397	1.391	1.369	C2-C1-C6	120.282	120.191	121.0
C1-C6	1.398	1.393	1.394	C2-C1-C7	121.520	121.625	
C1-C7	1.482	1.480	1.464	C6-C1-C7	118.199	118.184	119.8
C2-C3	1.402	1.396	1.400	C1-C2-C3	120.688	120.788	120.6
C2-H11	1.086	1.082		C1-C2-H11	119.509	119.524	
C3-C4	1.415	1.410	1.402	C3-C2-H11	119.803	119.688	
C3-N12	1.377	1.375		C2-C3-C4	119.388	119.295	119.0
C4-C5	1.397	1.391	1.412	C2-C3-N12	120.075	120.200	
C4-C15	1.503	1.499		C4-C3-N12	120.537	120.505	
C5-C6	1.391	1.385	1.379	C3-C4-C5	118.646	118.699	119.8
C5-H19	1.088	1.084		C3-C4-C15	120.182	120.124	
C6-H20	1.084	1.081		C5-C4-C15	121.172	121.177	
C7-O8	1.216	1.207		C4-C5-C6	122.185	122.153	121.0
C7-O9	1.357	1.355		C4-C5-H19	118.426	118.432	
O9-H10	0.970	0.966		C6-C5-H19	119.389	119.415	120.0
N12-H13	1.004	1.000		C1-C6-C5	118.812	118.874	119.6
N12-H14	1.005	1.001		C1-C6-H20	119.516	119.467	
C15-H16	1.099	1.095		C5-C6-H20	121.672	121.659	
C15-H17	1.099	1.095		C1-C7-O8	125.144	125.110	115.1
C15-H18	1.093	1.089		C1-C7-O9	113.457	113.445	
				O8-C7-O9	121.400	121.445	
				C7-O9-H10	105.975	105.652	
				C3-N12-H13	121.667	121.445	
				C3-N12-H14	120.575	120.545	
				H13-N12-H14	117.758	118.011	
				C4-C15-H16	111.722	111.646	
				C4-C15-H17	111.722	111.646	
				C4-C15-H18	111.000	111.006	
				H16-C15-H17	107.388	107.280	
				H16-C15-H18	107.388	107.521	
				H17-C15-H18	107.388	107.521	

Note : bond lenth are Å bond angle are degrees.
[a] The X-Ray data from refs (16,17)

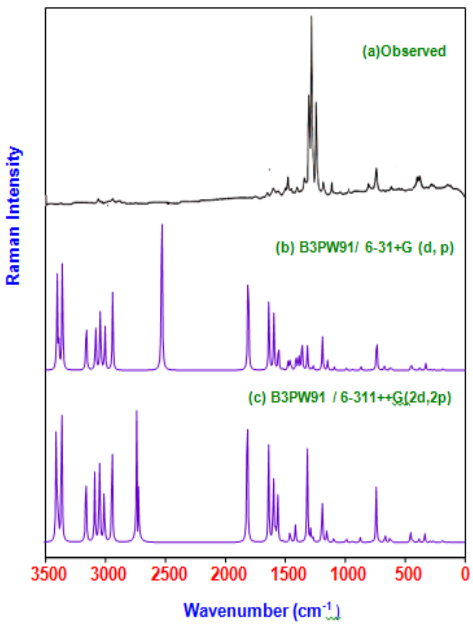

Fig 3. FT –Raman spectrum of 3-amino-4-methyl benzoic acid.

The calculated geometrical parameters represent a good approximation and they are the bases for the calculating other parameters, such as vibrational frequencies and thermodynamics properties. The comparative graphs of bond lengths, bond angles and dihedral angles of AMBA for two sets are presented in Figs. 6–8, respectively. The COOH bond length calculated , C2–C3 (1.402 A˚) is lengthened by 0.011 A˚ to the bond length C5–C6 (1.391 A˚). From the above, it is clear that the lengthening of C–C bond lengths in the ring are exactly at the substitution place and these differences of bond lengths are reversed in the experimental values [17]. The bond length of C O calculated by B3PW91/6-31+G(d,p) /6-311++G(2d,2p) are 1.216 A˚ and 1.207 A˚ , respectively. By comparing these values with experimental value of 1.202 A˚ , it is seen that the B3PW91/6-311++G(2d,2p) method under estimates the bond length whereas the DFT B3PW91/6-31+G(d,p) method overestimates the same.

4.2. Vibrational assignments

The AMBA consists of 20 atoms and belongs to Cs symmetry. Hence the number of normal modes of vibrations for AMBA works to 54 Of the 54 normal modes of vibrations, 37 modes of vibrations are in plane and remaining17 are out of plane. The bands that belong to the in- plane modes are represented as A' while the out-of-plane modes as A" . Thus the 54 normal modes of vibrations of AMBA are distributed as

Vib = 37A + 17A . All the 54 fundamental vibrations are active in both Raman scattering and IR absorption. The harmonic vibrational frequencies are calculated for Toluic acid using DFT methods and utilizing the triple split valence basis set along with the diffuse and polarization functions, B3PW91/6-31+G(d,p) and B3PW91/6-311++G(2d,2p) observed FT- IR and FT-Raman frequencies for various modes of vibrations. They are presented in Table 2.

Table 2. Vibrational spectral analysis of 3-amino-4-methyl benzoic acid based on B3PW91/ 6-31+G (d, p) and

No	Spe	Observed frequency (cm^{-1})		Calculated frequency (cm^{-1})				IR intensity		Raman activity		Vibrational assignments/(%)PED
				Unscaled		Scaled						
		FT-IR	FT-Raman	A	B	A	B	A	B	A	B	
1	A'	3401		3799	3800	3403	3400	94.19	96.88	150.63	143.65	νOH(100)
2	A'	3386		3798	3785	3388	3385	42.71	38.89	36.02	33.89	$\nu_{ass}NH_2$(99)
3	A'	3356		3668	3662	3359	3355	59.17	57.24	167.24	165.46	$\nu_{ss}NH_2$(99)
4	A'	3152		3238	3223	3160	3153	1.40	1.43	88.59	87.27	νCH(98)
5	A'		3079	3214	3200	3082	3080	4.61	4.25	71.62	67.80	νCH(98)
6	A'		3039	3189	3174	3043	3040	15.96	13.56	99.46	94.04	νCH(96)
7	A'	2999		3143	3129	3004	3001	11.65	10.30	62.24	56.49	$\nu_{ass}CH3$(98)
8	A"		2934	3079	3063	2940	2935	18.38	16.30	104.23	103.57	$\nu_{ass}CH3$(98)
9	A'			3024	3018	2730	2725	36.98	32.13	276.23	302.92	$\nu_{ss}CH3$(98)
10	A'			1808	1793	1810	1809	401.54	396.27	135.72	126.94	νCO(66),bOH(24),bCC(12)
11	A'		1632	1676	1665	1637	1631	147.76	137.34	70.59	66.62	νCC(65),bCH(18),NH_{2sciss}(14)
12	A'		1592	1653	1646	1595	1591	121.73	89.44	58.03	52.69	NH_{2sciss}(65),bCH(18)bCC(10)
13	A'		1553	1632	1623	1557	1555	21.83	33.94	29.51	33.11	νCC(68),bCC(20),bCH(12)
14	A'		1513	1554	1549	1520	1513	49.93	44.77	1.27	0.87	bCH(68),bCN(17), νCC(11)
15	A'		1474	1504	1501	1477	1473	23.00	19.65	7.98	7.88	bCH_{3ipb}(88)
16	A"	1455		1486	1483	1461	1454	9.43	7.87	10.82	7.10	bCH_{3opb}(84)
17	A'		1447	1465	1459	1449	1446	40.21	40.93	2.74	1.81	νCN(72),νCC(14),bCH(10)
18	A'	1406	1404	1412	1408	1410	1408	4.57	1.75	16.69	12.12	bCH_{3sb}(85)
19	A'	1382		1394	1384	1388	1380	3.21	143.20	15.19	37.88	νCC(56),bCH(14),bCC(12),bCO(10)
20	A'		1355	1386	1373	1361	1353	212.24	27.14	35.10	0.25	νCO(70),νCC(16),bCH(12)
21	A'	1312	1311	1320	1316	1316	1310	40.31	35.27	22.26	25.58	bCH(66),νCN(23),bOH(10)
22	A'	1279	1279	1311	1312	1282	1280	4.22	17.92	1.80	8.36	bCH(68),bCC(19)
23	A'		1263	1285	1284	1266	1262	4.74	12.55	4.14	3.46	νCC(66),bCC(20),bOH(11)
24	A'	1186	1184	1195	1194	1190	1185	238.03	253.36	29.61	30.13	bOH(21),νCO(16),bCH(10)
25	A'	1142	1145	1156	1154	1147	1146	68.51	63.12	9.32	8.40	νCC(64),NH_{2rock}(20),νCC(10)
26	A'	1088		1118	1109	1091	1089	87.65	99.65	3.26	3.35	νCC(65),νCO(21),Bcc(11)
27	A"	101		1053	1053	1019	1014	2.37	1.70	0.12	0.21	CH_{3opr}(86)

28	A'	985		1050	1046	991	983	11.12	11.66	2.71	2.71	NH_{2rock}(83),νCC(12)
29	A'		934	1008	1008	940	935	20.49	26.28	0.99	0.87	CH_3ipr(85),NH_{2rock}(12)
30	A"	926		966	971	931	924	0.03	0.02	0.16	0.15	γCH(80),
31	A'	866		955	953	870	867	3.91	3.48	3.80	3.09	νCC(71),CH_{3ipr}(19)
32	A"		842	890	895	848	841	13.60	9.95	0.15	0.02	γCH(80)
33	A"	801		842	844	807	802	3.67	1.18	0.19	0.22	γCH(77),γ CC(16)
34	A"	769	766	775	777	772	770	75.34	72.73	0.45	0.40	γCH(76),γCC(14),γCO(10)
35	A'	735		771	770	738	734	0.81	0.97	31.95	33.05	νCC(77)
36	A'		671	724	728	675	670	33.74	0.19	4.69	0.38	bCO(76),b_{ring}(16)
37	A"	662		720	725	668	660	0.38	32.71	0.44	4.43	γring(70), γCH(12)
38	A'	622	622	625	627	627	621	27.22	25.34	2.78	2.73	bCO(66),b_{ring}(14)
39	A"		605	619	614	612	607	67.16	53.63	1.65	1.22	γOH(62), γring(19)
40	A'		447	555	556	451	449	0.18	0.07	5.52	5.47	bCN(70),b_{ring}(12)
41	A"			550	548	438	436	20.53	22.25	1.34	1.21	γCO(66),$γ_{ring}$(11),γCH(10)
42	A'		420	524	524	427	422	10.33	9.87	0.60	0.47	b_{ring}(65),bCC(16)
43	A"			445	445	413	410	15.94	16.29	0.10	0.07	$γ_{ring}$(62)
44	A'			398	397	381	380	2.78	2.68	2.84	2.35	bCC(66),bCN(12),bCO(10)
45	A"			395	395	379	377	1.28	0.64	0.02	0.02	NH_{2twist}(58)
46	A'			351	351	329	330	3.20	2.75	5.22	4.79	bCC(66),b_{ring}(13)
47	A'			308	305	289	285	1.38	1.40	0.76	0.89	b_{ring}(66)
48	A"			291	290	263	259	4.42	3.31	0.74	0.80	γCO(58)
49	A"			209	206	191	189	2.17	2.14	0.26	0.35	γCN(56),$γ_{ring}$(18)
50	A"			190	188	186	182	0.44	0.44	1.24	0.92	CH_{3twist}(54),$γ_{ring}$(16)
51	A'			177	178	165	166	0.61	0.63	0.23	0.25	b_{ring}(61)
52	A"			133	130	129	127	0.84	0.72	0.27	0.34	γCCH_3ipr(58),γC-COOH(19)
53	A"			95	90	89	88	0.53	0.57	0.09	0.08	γC-COOH(54),$γ_{ring}$(17)
54	A"			60	52	54	54	208.74	176.42	0.08	0.00	$NH2_{wagg.}$(56)

A’			4153	3751	166.30	121.61	50.25	71.13
A’			3403	3234	4.57	1.40	42.97	70.94
A’	3186	3152	3399	3227	0.90	5.76	60.14	49.16
A’	3140	3055	3238	3011	44.00	52.33	98.16	122.16
A’	1860	1681	1974	1765	363.52	273.43	91.49	122.27
A’	1802		1792	1634	64.93	56.69	53.88	70.96
A’	1767	1597	1776	1617	8.11	9.20	13.06	17.51
A’	1605	1500	1620	1487	295.55	254.47	2.69	4.23
A’	1570	1444	1562	1446	5.01	25.41	4.45	8.30
A’	1500		1546	1426	59.68	52.95	1.98	3.75
A’	1430	1333	1424	1363	138.62	80.43	2.04	2.80
A’	1372		1394	1288	48.95	57.91	23.61	28.50
A’	1326	1278	1323	1268	62.16	82.33	15.67	2.54
A’	1291	1194	1286	1217	69.50	67.58	3.21	24.59

Comparison of frequencies calculated at DFT with the experimental values reveal the overestimation of the calculated vibrational modes due to the neglect of anharmonicity in real system. Inclusion of electron correlation in the density functional theory to certain extent makes the frequency values smaller in comparison with the DFT frequency data.

Although basis set are marginally sensitive as observed in the DFT values using /6-31+G(d,p) /6-311++G(2d,2p), reduction in the computed harmonic vibrational frequencies are noted. With out affecting the basic level of calculations, it is customary to scale down the calculated harmonic frequencies in order to develop an agreement with the experimental values. The scaled calculated frequencies minimize the rootmean square difference between calculated and experimental frequencies for bands with definite identifications. The descriptions concerning the assignment have also been indicated in Table 2. The comparative IR and Raman spectra of experimental and calculated are given in Figs. 2 and 3, respectively

C–H vibrations

The carbon-hydrogen stretching vibrations give rise to bands in the region 3000–3100 cm^{-1} in all the aromatic compounds [18,19]. Since the AMBA are disubstituted aromatic system, it has three adjacent C–H moieties. The expected four C–H vibrations corresponds to stretching modes of C5–H19, C6–H20, and C6–H11 units. These vibrations are assigned at 3160, 3082and 3043 cm^{-1} 3153, 3080 and 3020 cm^{-1} are in agreement with computed frequencies by B3PW91/6-31+G(d,p) /6-311++G(2d,2p) as well as literature data.

The C–H in-plane bending mode usually appears in the range of 1300–950 cm^{-1} and C–H out-of-plane bending vibrations in the region 950–670 cm^{-1} [20,21]. In the present case, the C–H in-plane and C–H out-of-plane bending vibrations are observed at 1280, 1310, 1120 and d , 8414, 802 and 770 cm^{-1} , respectively. These assigned vibrations are in the expected region and agree quite well with the calculated frequencies by B3PW91/6-311++G(2d,2p) method.

CH_3 vibrations

The C–H stretching vibrations of the methyl group are normally falling in the region 2840–2975 cm^{-1} [22,23]. There are two strong bands around 2960 cm^{-1} and a strong band around 2890 cm^{-1} corresponding to asymmetric and symmetric stretching modes, respectively [24,25]. In the present molecule, two strong bands are assigned in FTIR at 2999 and 2934 cm^{-1} in FT-Raman spectrum. The theoretically computed values by B3PW91/6-311++G (2d,2p) method for CH_3 stretching are approximately coincide with FT Raman experimental values. The C–H in-plane and out-of-plane bending vibrations for methyl group in the AMBA are assigned in FTIR 1455 cm^{-1} and 14774 cm^{-1}in FT-Raman spectrum, respectively. These assignments are in line with the literature values [26,27] and coincide with the calculated frequencies by B3PW91/6-311++G(2d,2p) (with scaling). The C–CH3 stretching, in-plane and out-plane bending vibrations for AMBA are assigned at 129 and 127 , respectively. The theoretically computed frequencies for C–CH3 vibrations by B3PW91/6-31+G(d,p) /6-311++G(2d,2p) method shows excellent agreement with recorded spectrum as well as with literature values [28].

C- NH2 vibrations

The asymmetric frequency calculated at B3PW91using 6-31+G(d,p) /6-311++G(2d,2p) falls in the range 3292–3585 cm^{-1} . Inspection of these shows that one calculated at 3583 cm^{-1} (after scaling down) at) B3PW91/6-311++G(2d,2p) seems to be in satisfactory agreement with a very strong FTIR band at 3386 cm^{-1} . Even though it is overestimated due to neglect of anhormonicity, it is very nearer to the reported value of 3500 cm^{-1} for phenylamine [29]. The same trend is not reflected when we look at the NH2 symmetric stretching frequency, the reported value of 3355 cm^{-1} for phenylamine is 145 cm^{-1} higher than the scaled value at B3PW91 /6-311++G(2d,2p) .

The calculated C-NH2 stretching at 1446 cm^{-1} by B3PW91 /6-311++G(2d,2p) method coupled with in-plane bending of CH exactly coincides when we compare with the reported range of 1250–1340 cm^{-1} [30]. The computed NH2 scissoring vibration at 1595 cm^{-1} and 1591 cm^{-1} by B3PW91/6-31+G(d,p) /6-311++G(2d,2p) is in satisfactory agreement with the expected characteristic value, 1600 cm^{-1} [29]. This is also in very good agreement with the recorded strong band in FTIR at 1626 cm^{-1} . The NH2 scissoring mode also contributes to C-C stretching mode at 1632 cm^{-1} . This is in excellent agreement with the earlier works [31,32]. The C-NH2 out-of-plane and in-plane bending vibrations at 451,459 and 191,189cm^{-1} respectively, are also in good agreement with the assignment in the experimental data. The NH2 wagging computed at 668 cm^{-1} by B3LYP/6-311++G(d,p) method exactly matches with FTIR value at 671 cm^{-1} . The NH2 rocking vibration calculated to be 985 cm^{-1} by B3PW91 /6-311++G(2d,2p) method deviates negatively by 20 cm^{-1} when we compare with the experimental FT-Raman data.

CC Vibrations

The aromatic ring vibrational modes of title compound have been analyzed based on the vibrational spectra of previously published vibrations of the benzene molecule is helpful in the identifications of the phenyl ring modes [33,34]. The ring stretching vibrations are very prominent, as the double bond is in conjugation with the ring, in the vibrational spectra of benzene and its deriva tives [35]. The ring carbon–carbon stretching vibration occurs in the region of 1650–1200 cm^{-1}. In general, the bands are of variable intensity and are observed at 1625–1590, 1590–1575, 1540–1470, 1465–1430 and 1380–1280 cm^{-1} from the frequency ranges given by Varsanyi [36] for the five bands in the region. In the present study, the wavenumbers observed in the FTIR spectrum at 1382, 1142, 1088, 866, and 735 cm^{-1} are assigned to CAC stretching vibrations. The same vibrations appear in the FT-Raman spectrum at 1553, 1263 and 1145cm^{-1}. The calculated carbonyl stretching is calculated as about 1632 cm^{-1}, but due to the intra- and intermolecular hydrogen bonding this mode is observed at Raman spectra of the title molecule. The computed wavenumber for CC stretching vibrations are found in the range of 1649–851 cm^{-1} (mode Nos. 10,13,19,23,25-26) by B3Pw91/6-311++G(d,p) and in the range of 1645–875 cm^{-1} by P3PW91/6-311++G(2d,2p) method. The observed values are in good correlation with the literature data of 1622, 1427, 1341, 1325, 1278, 1258, 1122 cm^{-1} [37] and calculated values. The PED corresponding to some these vibrations are mixed mode of contributing 80%. The in-plane deformation vibrations are at higher wavenumbers than out-of-plane vibrations. Shimanouchi et al.

[38] gave the frequency data for these vibrations for different benzene derivatives as a result of normal coordinated analysis. For aromatic ring, some bands are observed below 700 cm^{-1}, these bands are quite sensitive to change in the nature and position of the substituent's [39,40]. Although other bands depend mainly on the substitution and the number of substituent rather than on their chemical nature or mass, so that these latter vibrations, together with the out-of-plane vibrations of the ring hydrogen atoms are extremely useful in determining the positions of substituent's. The predicted wavenumbers of CCC in plane bending and out-of-plane bending vibrations are also in good agreement with the measured values and literature data [40].

-COOH vibrations

The most characteristic feature of carboxylic group is a single band observed usually in the range 1690–1655 cm^{-1} region [41,42] and this band is due to the C= O stretching vibration. The very strong band appearing at 1632 cm−1 in FT-Raman is assigned to C=O stretching vibration. This is in agreement with our earlier report [43]. The OH stretching band is characterized by very broadband appearing near about 3400 cm^{-1} [44]. The band observed at 3401 cm^{-1} in FT-IR spectrum is assigned to O–H stretching vibration.

The O–H in-plane and out-of-plane bending vibrations are usually observed in the regions 1350–1200 cm^{-1} and 720–590 cm^{-1} [45,46]. In AMBA the O–H in-plane bending vibrations are found at 1186 cm^{-1} in FT-IR and 1184 cm^{-1} in FT-Raman spectrum and 605 cm^{-1} in FT-Raman spectrum is assigned to O-H out plane bending vibrations, respectively. These assignments are in line with the literature values. The C-O stretching vibration is normally observed at 1310-1210 cm^{-1} due to C-O stretching vibration.A strong intense band at 1312 cm^{-1} in FT-IR and 1311 cm^{-1} in FT-Raman spectra corresponding to the computed wavenumber 1316 cm^{-1} and 1310 cm^{-1} is assigned to the C–O stretching mode which is a pure mode. From the above observation, it is clear that the assigned band is in the expected region [47] and in good agreement with computed values . The predicted wave numbers of C–O in-plane and out-of-plane bending are good agreement with literature values.

5. Natural bond orbital analysis

The natural bond orbital (NBO) [48] analysis of AMBA are being performed to estimate the delocalization pattern of electron density (ED) between the principal occupied Lewis-type (bond or lone pair) orbitals and unoccupied non-Lewis (antibond or Rydberg) orbitals. Table. 3 lists the occupancies and energies of most interacting NBO's along with their percentage of hybrid atomic orbital contribution.

The interactions result is a loss of occupancy from the localized NBO of the idealized Lewis structure into an empty non-Lewis orbital. For each donor (i) and acceptor (j), the stabilization energy E (2) associated with the delocalization from i → j is estimated as

$$E^{(2)}\Delta E_{ij} = q_i \frac{F(i,j)^2}{\varepsilon_j - \varepsilon_i}$$

where q_i is the donor orbital occupancy, ε_i and ε_j are diagonal elements and F (i,j) is the off diagonal NBO Fock matrix element. The NBO analysis provides an efficient method for studying intra and intermolecular bonding and also provides a convenient basis for investigating charge transfer or conjugative interaction in molecular systems [49].

The possibilities of ED delocalization from the lone pair donor atoms to the antibonding acceptor atoms of the title molecule are depicted in Table. 3 In other words, the delocalization of ED through donor to the acceptor of this type contributed predominantly to the stabilization of entire molecular system. This is due to the fact that greater the value of E (2), the more intensive is the interaction between electron donors and electron acceptors and the greater the extent of conjugation of the whole system.

Table 3. Second-order perturbation theory analysis of Fock Matrix in NBO basis of 3-amino-4-methyl benzoic acid.

Bond (A – B)	Type	ED	Acceptor (j)	Type	ED	$E^{(2)}$ (KJ/Md)
$C_1 – C_2$	BD	1.97206	$C_3 – N_{12}$	BD*	4.14	0.02080
$C_1 – C_6$	BD	1.97415	-	-	-	-
$C_1 – C_6$	BD	-	$C_7 – O_9$	BD*	1.20	0.09139
$C_1 – C_7$	BD	1.97450	$C_7 – O_8$	BD*	18.96	0.01719
$C_2 – C_3$	BD	1.97319	$O_9 – H_{10}$	BD*	2.24	0.01053
$C_3 – N_{12}$	BD	1.98895	$N_{12} – H_{13}$	BD*	2.20	0.00724
$C_4 – C_5$	BD	1.97333	$C_4 – C_5$	BD*	2.44	0.02236
$N_{12} – H_{13}$	BD	1.98208	$C_1 – C_6$	BD*	23.16	0.0242
$N_{12} – H_{14}$	BD	1.98209	$C_2 – C_3$	BD*	3.52	0.02678
$O_9 – H_{10}$	BD	1.98757	$C_2 – C_3$	BD*	3.50	0.02675
$C_7 – O_8$	BD	1.99608	$C_1 – C_7$	BD*	2.55	0.07016
$C_{15} – H_{16}$	BD	1.97980	$C_1 – C_6$	BD*	3.04	0.02042
$C_{15} – H_{17}$	BD	1.97987	$C_4 – C_5$	BD*	3.04	0.02230
$C_{15} – H_{18}$	BD	1.99033	$C_4 – C_5$	BD*	3.70	0.02236
LP(1) O_8	BD	1.98018	$C_1 – C_7$	BD*	2.81	0.07016
LP(1) O_9	BD	1.97866	$C_7 – O_8$	BD*	5.98	0.01719
LP(1) N_{12}	BD	1.96455	$C_3 – C_4$	BD*	7.72	0.03722

The natural charges determined by natural bond orbital (NBO) analysis by B3PW91/6-31+G(d,p) method is presented in the Table. 3 The more negative charges on C1and C7 carbon atoms are due to the attachment of bromine atoms with these carbon atoms. When compared the charges of the aromatic ring carbon atoms, less negative charge is observed in the carbon atoms which has CH2Br group. This is caused by effect of bromine atom. The bromine atom Br10 has less negative charge than the carbon atoms C1 and C7. This is due to the hyper conjugative effect of the bromomethyl groups.

The hybrid directionality and bond bending analysis of the benzene ring in the title molecule provide excellent evidence to the substituent effect and steric effect. The angular properties of the natural hybrid orbitals are very much influenced by the type of substituent that causes conjugative effect or steric effect [50]. In Tabl. 3, the bending angles of different bonds are expressed as the angle of deviation from the direction of the line joining two nuclear centers. The σ*(C1–C2) bond is more bent away from the line of C1–C7 centers by 3.1° results a strong charge transfer path towards CH2Br. According to the results, we can say that the degree of pyramidalization has affected by CF3 substituents.

6. Analysis of Molecular electrostatic potential (MEP) surface.

The MEP surface generally provides information regarding the chemical reactivity of a molecule. The electrostatic

potential generated in space around a molecule by the charge distribution is helpful to understand how much electrophilic or nucleophilic the molecular species [51].

The electrostatic potential $V(\vec{r})$ at any point in space around a molecule by charge distribution is given by

$$V(\vec{r}) = \sum_A \frac{Z_A}{\left|\vec{R}_A - \vec{r}\right|} - \int \frac{\rho(\vec{r}')\,dr'}{\left|\vec{r}' - \vec{r}\right|}$$

Where $\rho(\vec{r}')$ is the electron density function of the molecule, ZA is the charge on the nucleus A located at $\vec{R}_A$ and $\vec{r}$ is the dummy integration variable. $V(\vec{r})$ is a real physical property, which can be determined either computationally or experimentally by diffraction methods [52].

Fig.4 shows the plot of MEP surface of AMBA along with the computationally derived electrostatic potential and electrostatic point charges on its individual atoms. It is clear from the figure that the atoms C7, H8 and H9 hold significant positive charges. In the colour scheme of MEP, the intensity of which is proportional to the absolute value of the potential energy. On the other hand, the positive electrostatic potentials are appeared as blue and the Green indicates surface areas where the potentials are closer to zero. In view of this, we can say that the delocalization of charge and electron density of atoms are primarily taking place within the benzene ring and the electron withdrawing Amino and methyl substituents are increasing the chemical reactivity of a molecule.

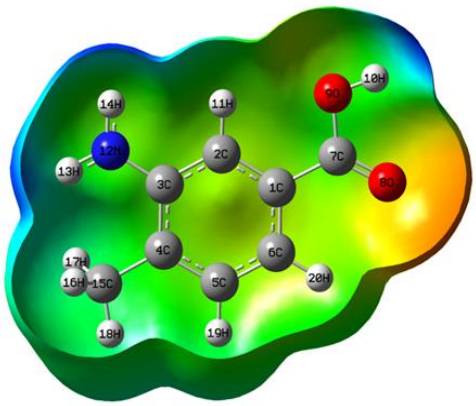

Fig 4. Electrostatic surfaces potential of 3-amino-4-methyl benzoic acid.

7. Frontier molecular orbital's (FMOs)

The most important orbital's in molecule is the frontier molecular orbital's, called highest occupied molecular orbital (HOMO) and lowest unoccupied molecular orbital (LUMO). These orbitals determine the way of molecule interacts with other species. The frontier molecular energy gap helps to characterize the chemical reactivity and kinetic stability of the molecule. A molecule with a small frontier orbital gap is more polarizable and is generally associated with a high chemical reactivity, low kinetic stability and is also termed as soft molecule [53]. The low values of frontier orbital gap in 4TFMP make it more chemical reactive and less kinetic stable. The frontier molecular orbital's plays an important role in the electric and optical properties [54].

The conjugated molecules are characterized by a small highest occupied molecular orbital- lowest unoccupied molecular orbital (HOMO-LUMO) separation, which is the result of a significant degree of intramolecular charge transfer from the end-capping electron acceptor groups through π–conjugated path [55]. The 3D plot of the frontier orbital's HOMO and LUMO along with DOS spectrum of 4TFMP molecule is shown in Fig. 5. The positive phase is red and negative phase one is green (For interpretation of the reference to color in the text, the reader is referred to the web version of the article). Many organic molecules, conjugated π electrons are characterized by large values of molecular first hyperpolarizabilities, were analyzed by means of vibrational spectroscopy [56, 57]. In most cases, even in the absence of inversion symmetry, the strongest band in the FT-Raman spectrum is weak in the FT-IR spectrum vice versa. But the intramolecular charge transfer from the donor-acceptor group in a single-double bond conjugated path can induce large variations of both the dipole moment and the polarizability, making FT-IR and FT-Raman activity strong at the same time. The analysis of wavefunction indicates that the electron absorption corresponds to the transition from the ground state to the excited state and is mainly described by one. An electron excitation from the high occupied molecular orbital to the lowest unoccupied molecular orbital (HOMO- LUMO).

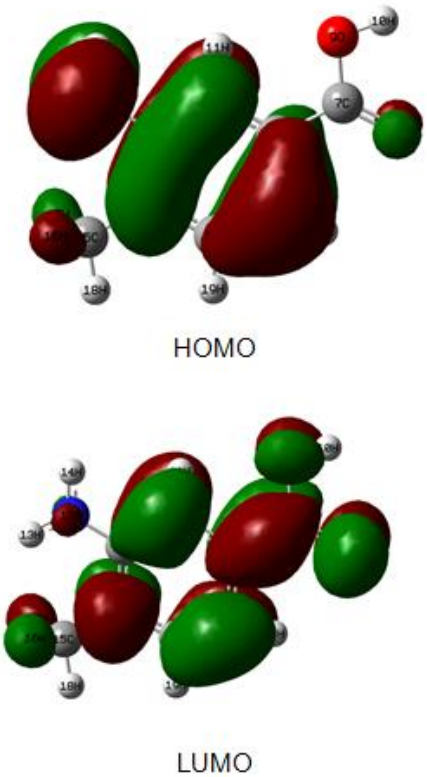

Fig 5. HOMO- LUMO of 3-amino-4-methyl benzoic acid.

Generally, the energy gap between the HOMO and LUMO decreases, it is easier for the electrons of the HOMO to be excited. The higher energy of HOMO, the easier it is for HOMO to donate electrons whereas it is easier for LUMO to accept electrons when the energy of LUMO is low.

HOMO energy = -0.28166 a.u
LUMO energy = 0.03867a.u
Energy gap = -0.24299 a.u

8. Mulliken atomic charge

Mulliken atomic charge calculation has an important role in the application of quantum chemical calculation to molecular system because of atomic charges effect dipole moment, molecular polarizability, electronic structure and more a lot of properties of molecular systems. The calculated Mulliken charge values of AMBA are listed in Table. 4 The

corresponding Mulliken atomic charge of C7 is 0.881e$^-$ for B3PW91/6-31+G(d,p) and 1.393e for B3PW91/6-311++G(2d,2p)

The charge on ring Nitrogen and Oxygen atoms exhibits a substantial negative charge, which are donar atoms.The Hydrogen atoms exhibits a positive charge, which is an acceptor atom.

9. Hyperpolarizability calculations

The polarizability α and the hyper polarizability β and the electric dipole moment μ of the AMBA were calculated by finite field method using B3PW91/6-31+G(d,p)/ 6-311++G(2d,2/p) basis set available in DFT package. To calculate all the electric dipole moments and the first hyper polarizabilities for the isolated molecule, the origin of the Cartesian coordinate system (x,y,z)=(0,0,0) was chosen at own centre of mass of AMBA.

The first hyperpolarizability (β0) of this noval molecular system and related properties (β, α0 and Δα) of AMBA are calculated and it is based on the finite-field approach. In the presence of an applied electric field, the energy of a system is a function of the electric field. First hyperpolarizability is a third rank tensor that can be described by a 3x3x3 matrix. The 18 components of the 3D matrix can be reduced to 10 components due to the Kleinman symmetry [58]. It can be given in the lower tetrahedral format. It is obvious that the lower part of the 3x3x3 matrixes is a tetrahedral. The components of β are defined as the coefficients in the Taylor series expansion of the energy in the external electric field. When the external electric field is weak and homogeneous, this expansion becomes:

$$E = E^0 - \mu_\alpha F_\alpha - \tfrac{1}{2}\alpha_{\alpha\beta}F_\alpha F_\beta - \tfrac{1}{6}\beta_{\alpha\beta\gamma}F_\alpha F_\beta F_\gamma + ...$$

where E0 is the energy of the unperturbed molecules, Fα is the field at the origin μα, ααβ and βαβγ are the components of dipole moment, polarizability and the first hyperpolarizability, respectively. The total static dipole moment μ, the mean polarizability α0, the anisotropy of the polarizability Δα and the mean first hyperpolarizability β0, using the x,y,z components they are defined as:

$$\mu = \left(\mu_x^2 + \mu_y^2 + \mu_z^2\right)^{1/2}$$

$$\alpha_0 = \frac{\alpha_{xx} + \alpha_{yy} + \alpha_{zz}}{3}$$

$$\alpha = 2^{-1/2}\left[\left(\alpha_{xx} - \alpha_{yy}\right)^2 + \left(\alpha_{yy} - \alpha_{zz}\right)^2 + \left(\alpha_{zz} - \alpha_{xx}\right)^2 + 6\alpha_{xx}^{\ 2}\right]^{1/2}$$

$$\beta_0 = \left(\beta_x^{\ 2} + \beta_y^2 + \beta_z^2\right)^{1/2}$$

$$\beta_x = \beta_{xxx} + \beta_{xyy} + \beta_{xzz}$$

$$\beta_y = \beta_{yyy} + \beta_{xxy} + \beta_{yzz}$$

$$\beta_z = \beta_{zzz} + \beta_{xxz} + \beta_{yyz}$$

The DFT B3PW91/6-31+G(d,p) /6-311++G(2d,2p) calculated first hyperpolarizability of AMBA 4.1489×10^{-30} and 3.870200×10^{-30} esu, are shown in Table. 5.

Table 4. Mulliken population analysis of 3-amino-4-methyl benzoic acid performed at B3PW91/ 6-31+G (d, p) and B3PW91 / 6-311++G(2d,2p).

Atoms	Atomic charges	
	B3PW91/ 6-31+G (d, p)	B3PW91 / 6-311++G(2d,2p)
C1	-0.869	-0.192
C2	0.664	-0.094
C3	-0.919	0.442
C4	1.553	-0.011
C5	-1.197	0.021
C6	-0.039	-0.151
C7	0.881	1.393
O8	-0.476	-0.839
O9	-0.460	-0.745
H10	0.387	0.297
H11	0.152	0.059
N12	-0.643	-0.715
H13	0.314	0.204
H14	0.318	0.205
C15	-0.519	0.065
H16	0.178	-0.025
H17	0.178	-0.025
H18	0.176	0.007
H19	0.147	0.028
H20	0.175	0.078

Table 5. The Ab initio B3PW91/ 6-31+G (d, p) and B3PW91 / 6-311++G(2d,2p) calculated electric dipole moments (Debye), Dipole moments compound, polarizability (in a.u), β components and βtot (10−30 esu) value of 3-amino-4-methyl benzoic acid.

Parameters	B3PW91 / 6-31+G (d, p)	B3PW91 / 6-311++G(2d,2p)	Parameters	B3PW91/6-31+G (d, p)	B3PW91 / 6-311++G (2d,2p)
μ_x	-3.751	-3.720	β_{xxx}	-21.182	-19.556
μ_y	2.187	2.162	β_{yyy}	16.697	16.697
μ_z	0.000	0.000	β_{zzz}	0.000	0.000
μ	4.342	4.302	β_{xyy}	-5.631	-5.209
α_{xx}	-57.953	-58.086	β_{xxy}	42.637	40.796
α_{yy}	-56.794	-56.781	β_{xxz}	0.000	0.000
α_{zz}	-68.276	-67.794	β_{xzz}	9.044	8.678
α_{xy}	4.693	4.605	β_{yzz}	2.579	2.602
α	-61.007667	-60.8870	β_{yyz}	0.000	0.000
Δα(esu)	$185.944 84\times10^{-25}$	$172.235 43\times10^{-25}$	βtot(esu)	$4.1489 56\times10^{-30}$	$3.8702 00\times10^{-30}$

Table 6. Statistical thermodynamic parameters of 3-amino-4-methyl benzoic acid at various temperatures.

Temp	Cp	(H-E)/T	(G-E)/T	S
100	19.526	9.703	-61.916	71.619
200	32.475	15.304	-72.862	88.166
300	44.140	23.032	-81.966	104.998
400	54.550	32.117	-90.205	122.323
500	63.317	42.176	-97.878	140.054
600	70.494	52.984	-105.104	158.088
700	76.375	64.390	-111.945	176.335
800	81.255	76.285	-118.441	194.726
900	85.354	88.585	-124.622	213.207
1000	88.830	101.223	-130.516	231.739

10. Thermodynamic properties

The total energy of a molecule is the sum of translational, rotational, vibrational and electronic energies. ie, E = Et + Er + Ev + Ee.

The statistical thermo chemical analysis of AMBA is carried out considering the molecule to be at room temperature of 298.15 K and one atmospheric pressure. The thermodynamic parameters, like rotational constant of the molecule by DFT method is presented in Table 6 for AMBA. The title molecule is considered as an asymmetric top having rotational symmetry number 1 and the total thermal energy has been arrived as the sum of electronic, translational, rotational and vibrational energies.

The variations in the zero point vibrational energy seem to be insignificant. The thermodynamic functions are determined from spectroscopic data by statistical methods. The thermodynamic quantities such as entropy Svib, enthalpy (H−E)/T, and Gibb's free energy (G–E)/T for various ranges (100K-1000K) of temperatures are determined using the vibrational wave numbers and these results are presented in the Table 6 The correlation equations between these thermodynamic properties and temperatures were fitted by parabolic formula. All the thermodynamic data provide helpful information for the further study on the title compound. From the Table 6 it can be observed that the thermodynamic parameters are increasing with temperature ranging from 100K to 1000K, (Fig. 6) due to the fact that the vibrational intensities of molecule with temperature. The regression coefficient is also given in the parabolic equation.

For DFT

$((H^0 - E_0^0)/T) = 1.915 + 0.111T - 0.000003T^2$ $(R^2=0.999)$

$((G^0 - E_0^0)/T) = -57.99 + 0.100T - 0.000003T^2$ $(R^2=0.999)$

$(S) = 59.90 + 0.211T - 0.0000009T^2$ $(R^2=1)$

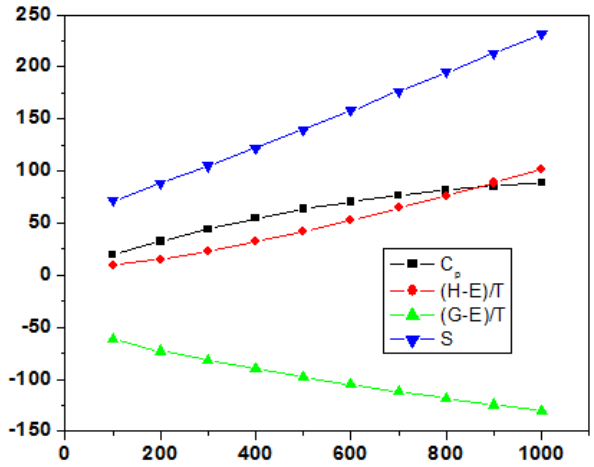

Fig 6. Thermodynamic parameters of 3-amino-4-methyl benzoic acid.

References

[1] H. Arslan, Ö. Algül, T. Önkol, Spectrochimica Acta 70A (2008) 606–614.

[2] M.C. Bermann, J.P. Bonte, I. Lesieur-Demarquilly, M. Debaert, D. Lesieur, M. Leinot, J. Benoit, C. Labrid, European Journal of Medical Chemistry 17 (1982) 85.

[3] K. Kreutz, A. Schlossberg, U.S. Patent 6,395,720 B1 (2002).

[4] Shou-Yihwang, C.Y. Chou, N.T. Liang, Journal of Raman Spectroscopy 19 (1988)365.

[5] K. Furic, J.R. Durig, Chemical Physics Letter 126 (1986) 92–96.

[6] G. Rauhut, P. Pulay, J. Phys. Chem. 99 (1995) 3093-3100

[7] A.P. Scott, L. Radom, J. Phys. Chem. 100 (1996) 16502-16513.

[8] Gaussian 09, Revision A.1, M. J. Frisch, G. W. Trucks, H. B. Schlegel, G. E. Scuseria, M. A. Robb, J. R. Cheeseman, G. Scalmani, V. Barone, B. Mennucci, G. A. Petersson, H. Nakatsuji, M. Caricato, X. Li, H. P. Hratchian, A. F. Izmaylov, J. Bloino, G. Zheng, J. L. Sonnenberg, M. Hada, M. Ehara, K. Toyota, R. Fukuda, J. Hasegawa, M. Ishida, T. Nakajima, Y. Honda, O. Kitao, H. Nakai, T. Vreven, J. A. Montgomery, Jr., J. E. Peralta, F. Ogliaro, M. Bearpark, J. J. Heyd, E. Brothers, K. N. Kudin, V. N. Staroverov, R. Kobayashi, J. Normand, K. Raghavachari, A. Rendell, J. C. Burant, S. S. Iyengar, J. Tomasi, M. Cossi, N. Rega, J. M. Millam, M. Klene, J. E. Knox, J. B. Cross, V. Bakken, C. Adamo, J. Jaramillo, R. Gomperts, R. E. Stratmann, O. Yazyev, A. J. Austin, R. Cammi, C. Pomelli, J. W. Ochterski, R. L. Martin, K. Morokuma, V. G. Zakrzewski, G. A. Voth, P. Salvador, J. J. Dannenberg, S. Dapprich, A. D. Daniels, Ö. Farkas, J. B. Foresman, J. V. Ortiz, J. Cioslowski, and D. J. Fox, Gaussian, Inc., Wallingford CT, 2009.

[9] P. Pulary, G. Fogarasi, G. Pongor, J.E. Boggs, A. Vargha, J.Am. Chem. Soc. 105 (1983) 7037−7047.

[10] T. Sundius. J.Mol. Struct. 218 (1990) 321−326.

[11] T. Sundius, Vib. Spectrosc. 29 (2002) 89–95.

[12] T. Sundius, Molvib (V7.0): Calculation of harmonic force fields and vibrational modes of molecules, QCPE program No: 807, 2002.

[13] P.L. Polavarapu, J. Phys. Chem. 94 (1990) 8106−8112.

[14] G. Keresztury, S. Holly, J. Varga, G. Besenyei, A.V. Wang, J.R. Durig, Spectrochim. Acta 49A (1993) 2007–2017.

[15] G. Keresztury, in: J.M. Chalmers and P.R. Griffiths (Eds), Handbook of Vibrational Spectroscopy vol.1, John Wiley & Sons Ltd,2002.

[16] Esma gunes ,cemal Parlak,Spectrochim.Acta 68A (2007)771-777.

[17] R.Montis,C.S Hook,P.N.Horton.M.B.Hursthouse.University of Southampton,crystal Structrue Report Archive, 2007.

[18] G. Socrates, Infrared Characteristic Group Frequencies, Wiley, New York, 1980.

[19] G. Varsanyi, Vibrational Spectra of Benzene Derivatives, Academic Press, New York, 1969.

[20] R.M. Silverstein, G.C. Basseler, C. Moril, Spectrometric Identification of Organic Compounds, John Wiley, New York, 1981.

[21] J. Coates, Interpretation of infrared spectra, a practical approach, in: R.A. Meyers(Ed.), Encyclopedia of Analytical Chemistry, John Wiley & Sons Ltd., Chichester,2000.

[22] N.B. Colthup, L.H. Daly, S.E. Wiberley, Introduction to Infrared and Raman Spec- troscopy, Academic Press, New York, 1990.

[23] F.R. Dollish, W.G. Fateley, F.F. Bentley, Characteristic Raman Frequencies of Organic Compounds, Wiley, New York, 1997.

[24] S. Ahmad, P.K. Verma, Indian Journal of Physics 64B (1990) 50.

[25] D. Sajan, K.P. Laladhas, I. Hubert Joe, V.S. Jayakumar, Journal of Raman Spec- troscopy 36 (2005) 1001.

[26] L.J. Bellamy, The Infrared Spectra of Complex Molecules, Chapman & Hall, Lon- don, 1975.

[27] N.B. Colthup, L.H. Daly, S.E. Wiberley, Introduction to Infrared and Raman Spec- troscopy, Academic Press Inc., London, 1964.
[28] S.B. Doddamani, A. Ramoji, J. Yenagi, J. Tonannavar, Spectrochimica Acta 67A (2007) 150–159.
[29] R.M. Silverstein, F.X. Webster, Spectrometric Identification of organic compounds, sixth ed., Wiley, 1988, p. 102.
[30] L.J. Bellamy, The Infrared Spectra of Complex Molecules, vol. 1, third ed., Chapman and Hall, London, 1975, pp. 93–287.
[31] R. Palanivel, R. Sethupathi, C. Rakkappan, G. Velraj, Asian Chem. Lett. 6 (2002) 1.
[32] S. Periyandy, S. Mohan, Proc. Natl. Acad. Sci. India 68A (IV) (1998) 435.
[33] N.B. Colthup, L.H. Daly, S.E. Wiberley, Introduction to Infrared and Raman Spectroscopy, Academic Press, New York, 1990.
[34] G. Socrates, Infrared Characteristic Group Frequencies, Wiley Interscience Publication, 1980.
[35] G. Varsanyi, Vibrational Spectra of Benzene Derivatives, Academic Press, New York, 1969.
[36] G. Varsanyi, Assignments of Vibrational Spectra of Seven Hundred Benzene Derivatives, vols. 1–2, Adam Hilger, 1974.
[37] Esma Gunes, Cemal Parlak, Spectrochim. Acta 82A (2011) 504–512.
[38] T. Shimanouchi, Y. Kakiutti, I.J. Gamo, Chem. Phys. 25 (1956) 1245–1252.
[39] R.J. Jakobsen, F.F. Bentely, Appl. Spectrosc. 18 (1964) 88–92.
[40] A.J. Mansingh, Chem. Phys. 52 (1970) 5896.
[41] C.B. Smith, Infrared Spectral Interpretation, CRC Press, New York, 1999.
[42] G. Socrates, Infrared and Raman Characteristic Group Frequencies, John Wiley, New York, 2001.
[43] J. Swaminathan, M. Ramalingam, V. Sethuraman, N. Sundaraganesan, S. Sebas- tian, Spectrochimica Acta Part A 73 (2009) 593.
[44] N. Sundaraganesan, B. Dominic Joshua, K. Settu, Spectrochimica Acta 66A (2007) 381–388.
[45] J. Coates, Interpretation of infrared spectra, a practical approach, in: R.A. Meyers (Ed.), Encyclopedia of Analytical Chemistry, John Wiley & Sons Ltd., Chichester,2000.
[46] S. Ahmad, S. Mathew, P.K. Verma, Indian Journal of Pure and Applied Physics 30 (1992) 764–770.
[47] N. Sundaraganesan, B. Dominic Joshua, Spectrochimica Acta 68A (2007) 771–777.
[48] G. Keresztury, S. Holly, J. Varga, G. Besenyei, A.V. Wang, J.R. Durig, Spectrochim. Acta 49A (1993) 2007–2017.
[49] M. Karabacak, L. Sinha, O. Prasad, Z. Cinar, M. Cinar, Spectrochim. Acta Part A 93 (2012) 33– 46.
[50] Ebrahimi, F. Deyhimi, H. Roohi, J. Mol. Struct. (Theochem) 626 (2003) 223–229.
[51] M. Karnan V. Balachandran M. Murugan M.K. Murali A. Nataraj Spectrochim. Acta116(2013)84-95
[52] P. Politzer, D.G. Truhlar, Eds. Chemical applications of atomic and molecular electrostatic potentials, plenum press, New York, 1981.
[53] B.J. Powell, T. Baruah, N. Bernstein, K. Brake, R.H. McKenzie, P. Meredith, M.R. Pederson, J. Chem. Phys. 120 (2004) 8608-8615.
[54] T.Karakurt,M.Dinçer,A. Çetin,M. S_ekerci, Spectrochim. Acta 77A (2010) 189-198.
[55] C.H. Choi, M. Kertesz, J. Phys. Chem. A 101 (1997) 3823-3831.
[56] Y. Ataly, D. Avci, A. Basoglu, J. Struct. Chem. 19 (2008) 239-246.
[57] T. Vijayakumar, I. Hubert Joe, C.P.R. Nair, V.S. Jayakumar, J. Chem. Phys. 343 (2008) 83-99.
[58] D.A. Kleinman, Phys. Rev. 126 (1962) 1977–1979.